

Supporting Information

Multivariate MOF-Templated Pomegranate-Like Ni/C as Efficient Bifunctional Electrocatalyst for Hydrogen Evolution and Urea Oxidation

Lu Wang, Lantian Ren, Xiaorui Wang, Xiao Feng, Junwen Zhou and Bo Wang*

Beijing Key Laboratory of Photoelectronic/Electrophotonic Conversion Materials, Key Laboratory of Cluster Science, Ministry of Education, School of Chemistry, Beijing Institute of Technology, Beijing 100081, P. R. China.

*Corresponding author. E-mail: bowang@bit.edu.cn.

Contents

Section A. Supplementary data (Figure S1-10, Table S1-2)

Section B. Supporting references

Section A. Supplementary data (Figure S1-10)

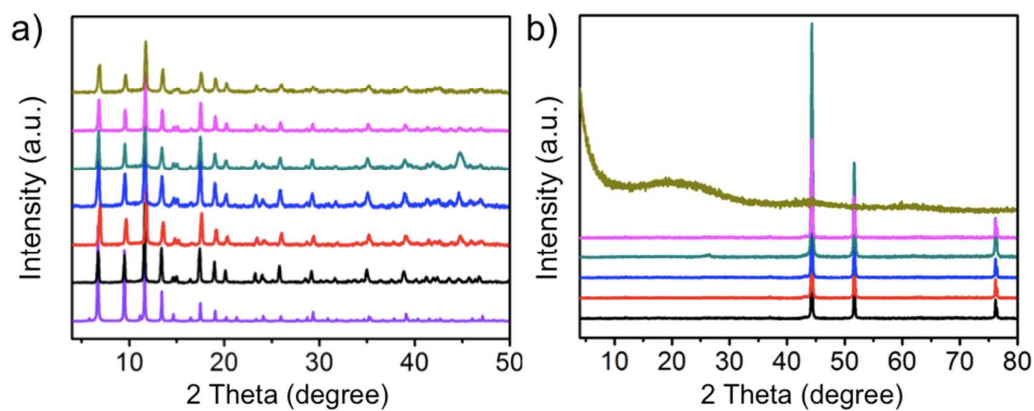


Figure S1. PXRD patterns of a) Zn/Ni-BTC with different Zn/Ni ratios and b) the derived Ni/C composites, respectively. Violet: simulated NiBTC, black: NiBTC, red: $\text{Zn}_{0.05}\text{Ni}_{0.95}\text{BTC}$, blue: $\text{Zn}_{0.2}\text{Ni}_{0.8}\text{BTC}$, dark cyan: $\text{Zn}_{0.5}\text{Ni}_{0.5}\text{BTC}$, magenta: $\text{Zn}_{0.8}\text{Ni}_{0.2}\text{BTC}$, dark yellow: ZnBTC.

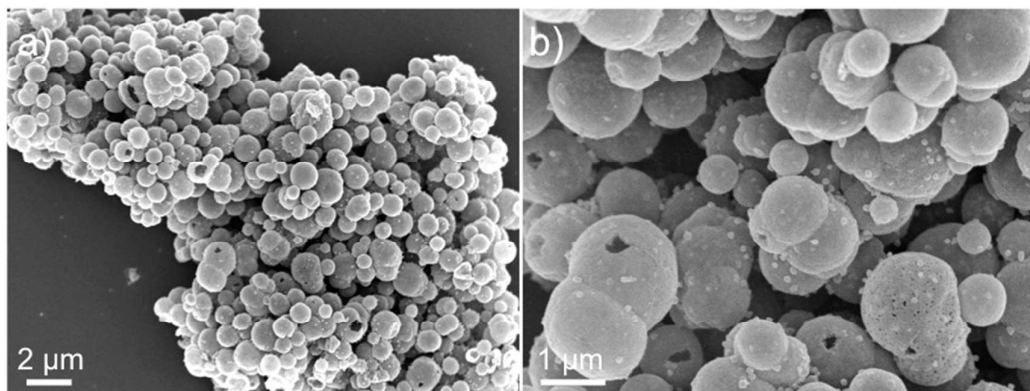


Figure S2. a, b) SEM images of Ni/C-0.

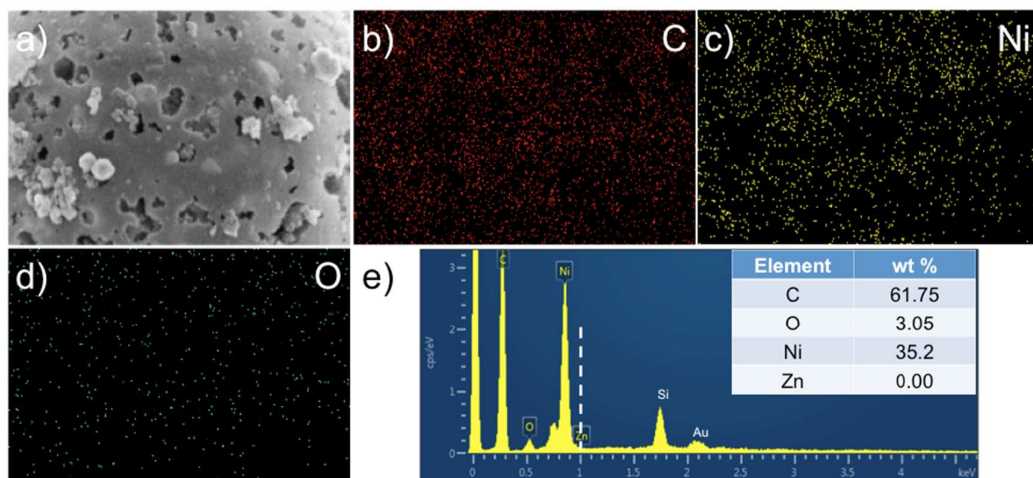


Figure S3. a-d) EDS elemental mapping images and e) EDX pattern of Ni/C-1.

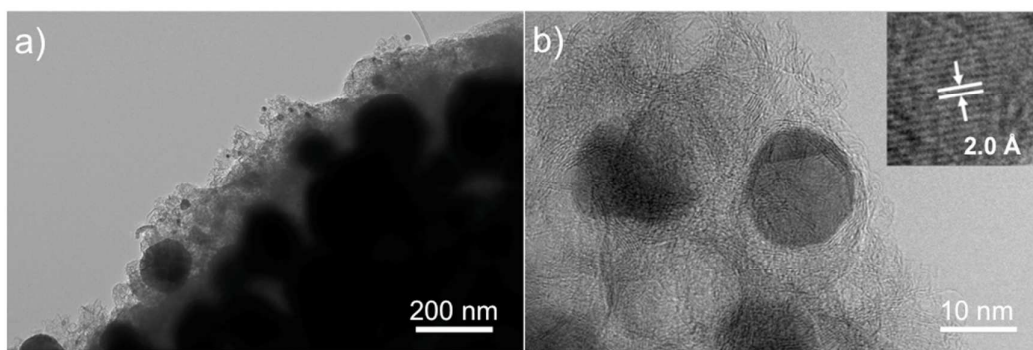


Figure S4. a) TEM image, b) HRTEM image of the edge of Ni/C-1 sphere.

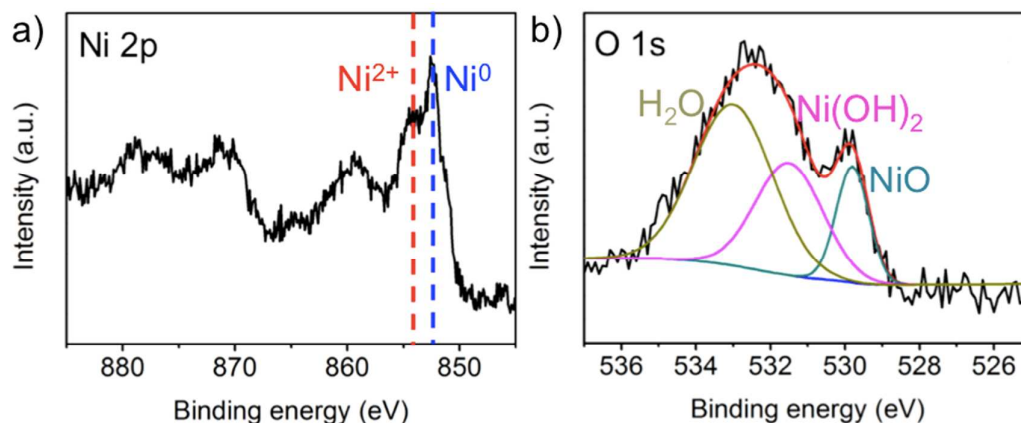


Figure S5. a) Ni 2p and b) O 1s high-resolution XPS spectra of Ni/C-1.

The peak at 854 eV is assigned to NiO, which could be formed during the exposure in air. According to previous reports, metallic nickel is highly active in ambient environments, with NiO and/or $\text{Ni}(\text{OH})_2$ forming spontaneously on the surface of atomically clean nickel metal. The two O 1s peaks at 529.8 and 531.5 eV are ascribed to NiO and $\text{Ni}(\text{OH})_2$ species, respectively. The component at 533.1 eV is associated with bound waters of hydration.¹

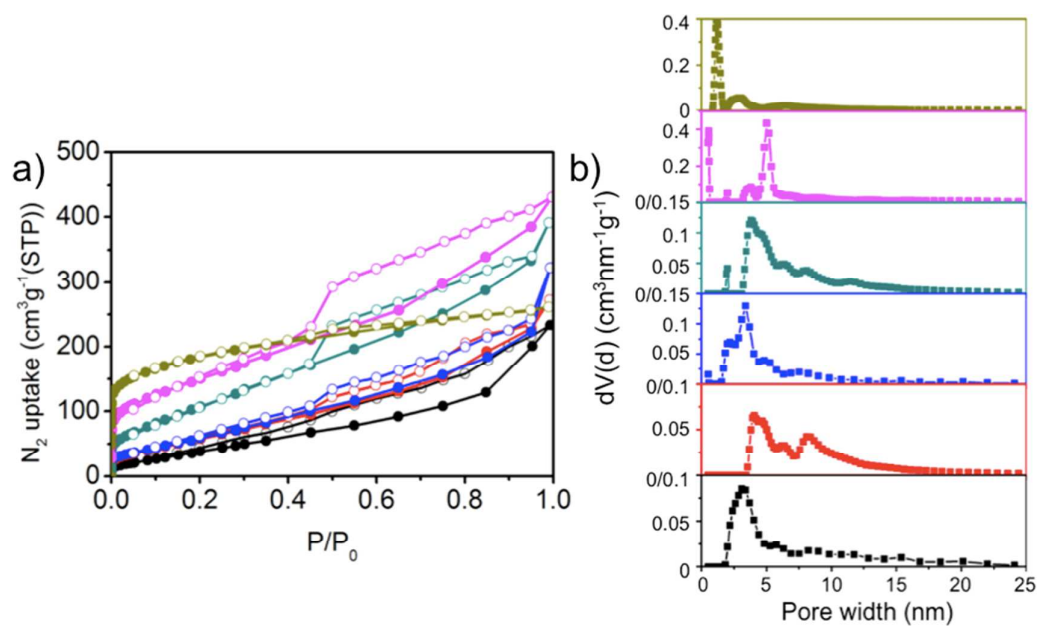


Figure S6. a) N₂ adsorption/desorption isotherms and b) pore size distribution patterns calculated based on NLDFT method of the Ni/C composites derived from the different MOF precursors, respectively. Black: NiBTC, red: Zn_{0.05}Ni_{0.95}BTC, blue: Zn_{0.2}Ni_{0.8}BTC, dark cyan: Zn_{0.5}Ni_{0.5}BTC, magenta: Zn_{0.8}Ni_{0.2}BTC, dark yellow: ZnBTC.

Table S1. Surface area and total pore volume of Ni/C composites derived from different MOF precursors, respectively.

MOF precursor	NiBTC	Zn _{0.05} Ni _{0.95} BTC	Zn _{0.2} Ni _{0.8} BTC	Zn _{0.5} Ni _{0.5} BTC	Zn _{0.8} Ni _{0.2} BTC	ZnBTC
surface area (m ² g ⁻¹)	182	250	255	438	545	663
total pore volume (cm ³ g ⁻¹)	0.2860	0.4217	0.4992	0.6050	0.6210	0.4045

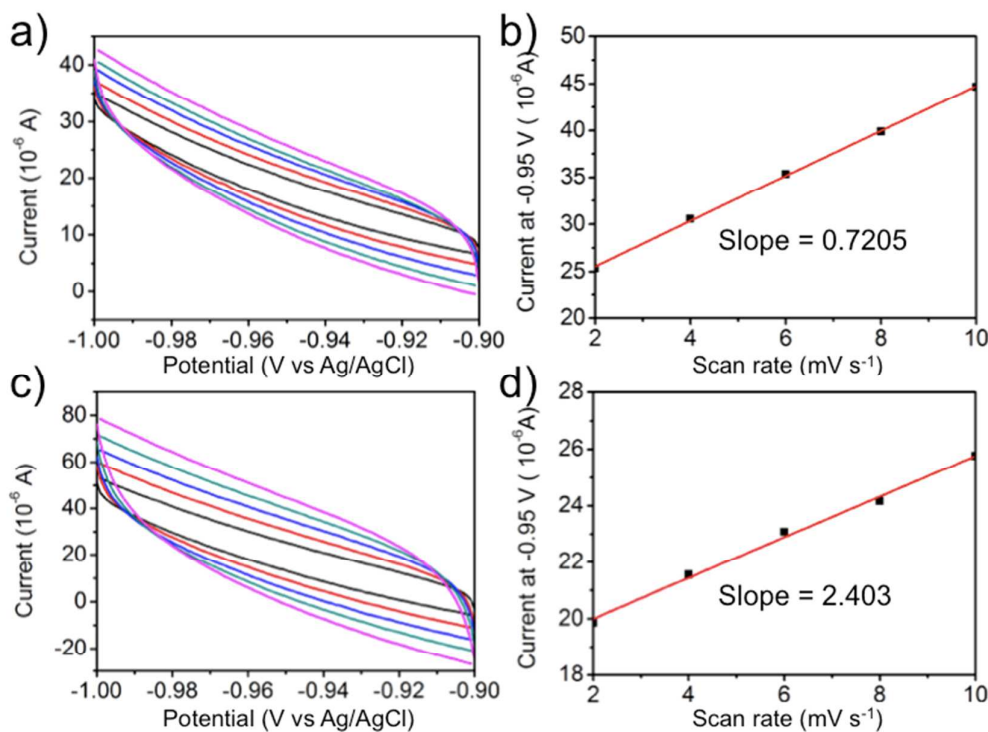


Figure S7. Cyclic voltammograms of a), Ni/C-0, c) Ni/C-1 measured in 1 M KOH in the non-Faradaic potential range from -0.9 V to -1.0 V versus Ag/AgCl at scan rates of 2 (black line), 4 (red line), 6 (blue line), 8 (green line) and 10 mV s^{-1} (pink line), respectively. Average capacitive current of b), Ni/C-0 and d), Ni/C-1 taken from center of potential window, at -0.95 V vs. Ag/AgCl.

In order to further explicate the HER activity of the electrode, we have conducted the analysis of electrochemical surface area (ECSA).

Electrochemical active surface area (ECSA) of the electrode was measured from the capacitive current associated with double-layer charging from the scan-rate dependence of cyclic voltammetry (CV). This measurement was performed on the same working electrodes within a small potential range of -0.9 V to -1.0 V versus Ag/AgCl and scan rates ranging from 2 to 10 mV s^{-1} . The relation between the charging current (i at the -0.95 V vs. Ag/AgCl), the scan rate (ν) and the double layer capacitance (C_{dl}) was given in equation 1.

$$i = \nu C_{dl} \quad (1)$$

Therefore, the slope of i as a function of ν gives a straight line with the slope equals to C_{dl} . The C_{dl} of Ni/C-0 and Ni/C-1 measured from the scan rate dependent CVs are 0.7205 mF cm^{-2} and 2.403 mF cm^{-2} , respectively.

The quasi-square shape CV is mainly caused by the complications from iR drop from the internal resistance of catalyst materials and the surface/electrolyte interface.^{2,}

3

Table S2. Comparison of HER performance in alkaline electrolyte of Ni/C-1 and other catalysts.

catalyst	loading density (mg cm ⁻²)	substrate	electrolyte	current density	overpotential	Tafel slope	reference
Ni/C-1	0.5	GCE	1 M KOH	10	40	77	This work
NiO/Ni-CNT	0.28	GCE	1 M KOH	10	80	82	Nat. Commun., 2014, 5, 4695
Zn0.30Co2.70S4	0.285	GCE	1 M KOH	10	85	-	J. Am. Chem. Soc. 2016, 138, 1359
KuCo@NC	0.2/5	GCE	1 M KOH	10	28	31	Nat. Commun. 2017, 8, 14969
Pt-Ni alloy	-	GCE	0.1 M KOH	10	65	78	Nat. Commun. 2017, 8, 15131
Pt NWs/SL-Ni(OH)2	-	GCE	0.1 M KOH	4	57.8	-	Nat. Commun. 2015, 6, 6430
			1 M KOH	4	85.5	-	
Pd-CNx	0.28	GCE	0.5 M KOH	5	180	150	ACS Catal. 2016, 6, 1929
Ni@NC	0.31	GCE	1 M KOH	10	205	160	Adv. Mater. 2017, 29, 1605057
Ni-MoS2	-	GCE	1 M KOH	10	98	60	Energy Environ. Sci., 2016, 9, 2789
Co-P/NC	1	GCE	1 M KOH	10	154	51	Chem. Mater. 2015, 27, 7636
CoP/rGO-400	0.28	GCE	1 M KOH	10	150	38	Chem. Sci. 2016, 7, 1690
Co-NRCNT	0.28	GCE	1 M KOH	10	370	-	Angew. Chem. Int. Ed. 2014, 53, 4372
Mo2C@N-C	0.28	GCE	1 M KOH	10	60	-	Angew. Chem. Int. Ed. 2015, 54, 10752
MoCx	-	GCE	1 M KOH	10	151	59	Nat. Commun. 2015, 6, 6512
40 wt% Pt on carbon black	0.8	GCE	1 M KOH	10	70	113	
Ni2P	0.38	GCE	1 M KOH	20	250	100	Phys. Chem. Chem. Phys., 2014, 16, 5917
CoOx@CN	0.12	GCE	1 M KOH	10	232	115	J. Am. Chem. Soc. 2015, 137, 2688
MoxC-Ni@NCVesicle	1.1	GCE	1 M KOH	10	126	93	J. Am. Chem. Soc. 2015, 137, 15753
beta-Mo2C nanotubes	0.75	GCE	0.1 M KOH	10	112	55	Angew. Chem. Int. Ed. 2015, 54, 15395
Ni1Mn1	-	GCE	0.1 M KOH	10	360	-	Adv. Funct. Mater. 2015, 25, 393
MoNi4/MoO2@Ni	43.4	nickel foam	1 M KOH	10	15	30	Nat. Commun. 2017, 8, 15437
NF-Ni3Se2/Ni	8.87	nickel foam	1 M KOH	10	203	79	Nano Energy 2016, 24, 103
MoO2 nanosheet	2.9	nickel foam	1 M KOH	10	27	41	Adv. Mater. 2016, 28, 3785
CuP-MNA-NF	-	nickel foam	1 M KOH	10	54	51	Adv. Funct. Mater. 2015, 25, 7337
Ni2P	-	nickel foam	1 M KOH	10	98	72	ACS Catal. 2016, 6, 714
Ni/NiP	11	nickel foam	1 M KOH	10	130	58.5	Adv. Funct. Mater. 2016, 26, 3314
h-NiSx-NF	142.2	nickel foam	1 M KOH	10	60	99	Adv. Energy Mater. 2016, 6, 1502333
NiFe/NiCo2O4/NF	-	nickel foam	1 M KOH	10	105	88	Angew. Chem. 2015, 127, 9483
Ni@NiO-Cr2O3	8	nickel foam	1 M KOH	100	150	-	Angew. Chem. 2015, 127, 12157
Ni0.89Co0.11Se2 MNS/NF	2.16	nickel foam	1 M KOH	10	85	52	Adv. Mater. 2017, 1606521
NiFe-LDH/Ni foam	-	nickel foam	1 M NaOH	10	210	-	Science 2014, 345, 1593
Co(OH)2@PANI HNSs/NF	-	nickel foam	1 M NaOH	10	88	91.6	Adv. Mater. 2015, 27, 7051
Ni5P4-Ni	3.475	nickel foil	1 M KOH	10	150	53	Angew. Chem. Int. Ed. 2015, 54, 12361
u-CoP/Ti	6.32	Ti	1 M KOH	10	60	49.1	J. Mater. Chem. A, 2016, 4, 10114
Ni0.33Co0.67S2 nanowires-Ti	0.3	Ti	1 M KOH	10	88	118	Adv. Energy Mater. 2015, 1402031
Ni-Mo on Ni	40	Ni	1 M KOH	400	110	-	Energy Environ. Sci., 2012, 5, 7869
Ni-Mo nanopowder	1	Ti	2 M KOH	20	70	-	ACS Catal. 2013, 3, 166
Fe-CoP/Ti	1.03	Ti foil	1 M KOH	10	78	75	Adv. Mater. 2017, 29, 1602441
CoP-Cu foil	-	Cu foil	1 M KOH	10	94	42	Angew. Chem. Int. Ed. 2015, 54, 6251
c-CoSe2/CC	-	carbon cloth	1 M KOH	10	190	85	Adv. Mater. 2016, 28, 7527
CoP/CC	0.92	carbon cloth	1 M KOH	10	209	129	J. Am. Chem. Soc. 2014, 136, 7587
2-Cylce NiFeOx	1.6	carbon fiber paper	1 M KOH	10	88	-	Nat. Commun. 2015, 6, 7261
MoB	2.3	no substrate	1 M KOH	10	225	59	Angew. Chem. Int. Ed. 2012, 51, 12703
Mo2C	0.8	no substrate	1 M KOH	20	210	54	
Pt electrode	-	no substrate	0.1 M KOH	1	30	70	Energy Environ. Sci. 2013, 6, 1509

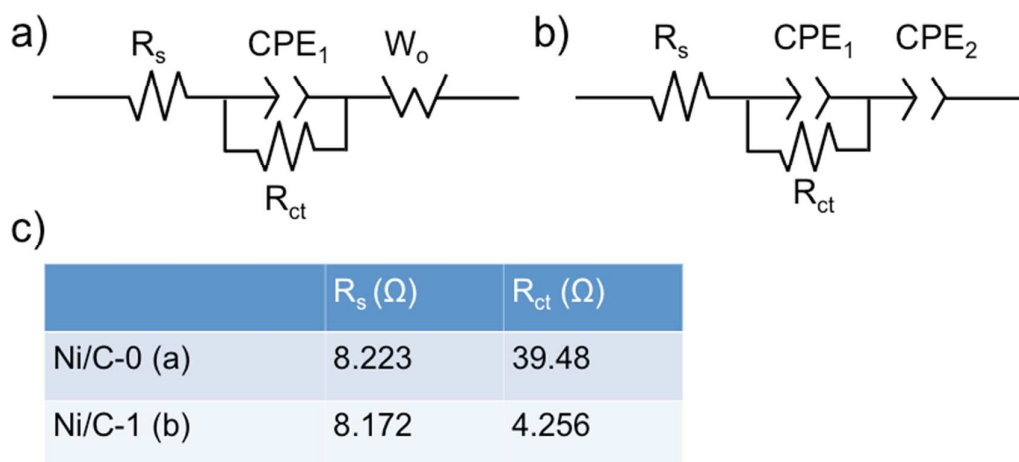


Figure S8. Equivalent electrical circuits of a) Ni/C-0 and b) Ni/C-1. c) Calculation result of series resistance (R_s) and charge transfer resistance at the Ni/C composite/electrolyte interface (R_{ct}) in the HER process in different electrolyte. CPE_1 and CPE_2 are the constant phase element. W_o is the Warburg element.

The R_{ct} of Ni/C-0 and Ni/C-1 in 1 M KOH are calculated to be 39.48 Ω and 4.256 Ω , respectively. The long tail of Ni/C-0 with the slope of 1 is attributed to the ion diffusion inside the electrode, resulting in the Warburg element, W_o . The tail of low frequencies of Ni/C-1 corresponds to a semi double-layer capacitance.⁴

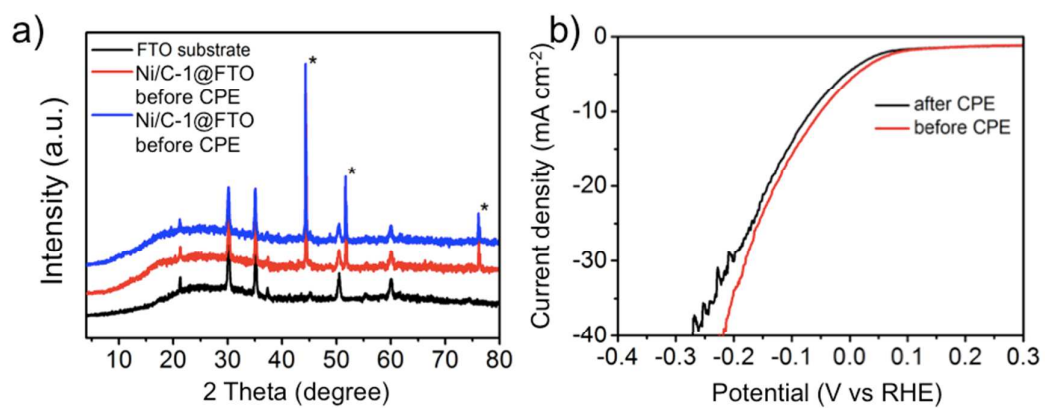


Figure S9. a) PXRD patterns and b) LSV curves of Ni/C-1@FTO before CPE and after CPE.

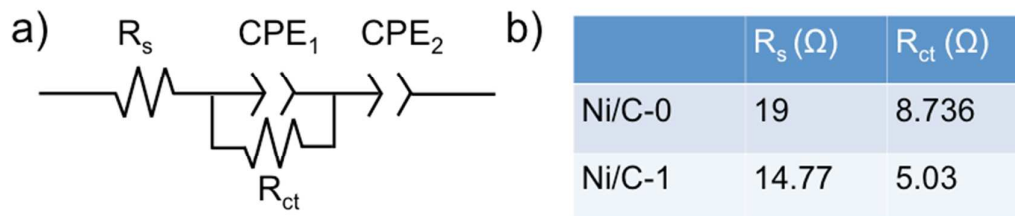


Figure S10. a) Equivalent electrical circuit of Ni/C-0 and Ni/C-1. b) Calculation result of series resistance (R_s) and charge transfer resistance at the Ni/C composite/electrolyte interface (R_{ct}) in the UOR process in 1 M KOH with 0.33 M urea. CPE₁ and CPE₂ are the constant phase element.

Supporting references

- (1) Zhao, S.; Yin, H.; Du, L.; He, L.; Zhao, K.; Chang, L.; Yin, G.; Zhao, H.; Liu, S.; Tang, Z. Carbonized Nanoscale Metal-Organic Frameworks as High Performance Electrocatalyst for Oxygen Reduction Reaction. *ACS Nano* **2014**, 8, 12660–12668.
- (2) L. M. De Silva; L. A. De Faria; Boodts, J. F. C. Determination of the morphology factor of oxide layers. *Electrochim. Acta* **2001**, 47, 395–403.
- (3) Li, Y.; Hasin, P.; Wu, Y. NixCo3–xO4 Nanowire Arrays for Electrocatalytic Oxygen Evolution. *Adv. Mater.* **2010**, 22, 1926–1929.
- (4) Hitz, C.; Lasia, A. Experimental study and modeling of impedance of the her on porous Ni electrodes. *J. Electroanal. Chem.* **2001**, 500, 213–222.